

Influence of Backbone Conformation on the Photoconductivity of Polydiacetylene Chains

Romano J. O. M. Hoofman, Gerwin H. Gelinck, Laurens D. A. Siebbeles, Matthijs P. de Haas, and John M. Warman*

Radiation Chemistry Department, IRI, Delft University of Technology, Mekelweg 15, 2629 JB Delft, The Netherlands

David Bloor

Department of Physics, University of Durham, Durham, DH1 3LE, United Kingdom

Received March 17, 2000; Revised Manuscript Received August 24, 2000

ABSTRACT: The thermochromic, solvatochromic, and photoconductive properties of 3-, 4-, 6-, and 9-BCMU (BCMU = poly(butoxycarbonylmethylurethane)-diacetylenes) resulting from changes from rod (red or blue) to coil (yellow) conformations of the polymer backbone have been studied. Photoexcitation of solutions of BCMUs in the rod state results in a large transient photoconductivity as monitored using the time-resolved microwave conductivity (TRMC) technique, while only very small conductivity signals are observed in the coil state. The thermochromic shift in going from the rod state at room temperature to the coil state at 65 °C is accompanied by a decrease in the photoconductivity. The large conductivity signal in the rod state is attributed to the formation of mobile charge carriers possibly via interchain charge transfer within aggregates. Values from 0.8×10^{-4} to 3×10^{-4} cm² V⁻¹ s⁻¹ are found for the lower limit to the product of the quantum efficiency for charge carrier formation, ϕ_p , and the sum of the charge carrier mobilities, $\Sigma\mu$. The decay of the photoconductivity is nonexponential and extends to microseconds.

Introduction

Since the first publication by Wegner,¹ a large number of polydiacetylenes have been synthesized and their physical properties measured. Polydiacetylenes (PDAs) have been extensively studied for their unique optoelectronic properties, such as dramatic thermochromic and solvatochromic changes^{2–6} and large nonlinear optical susceptibilities^{7–9} with ultrafast response times.⁸ The one-dimensional conjugated backbone combined with the structures of the side groups is responsible for these unique characteristics, which make PDAs potential candidates for photonic⁷ and electronic applications.^{10,11}

Since most of the early polydiacetylene derivatives were quite insoluble, the properties of their solutions received very little attention until a new class of PDAs was synthesized which showed relatively high solubility in both aqueous^{12,13} and nonaqueous solvents:^{14–17} the *n*-butoxycarbonylmethylurethane-PDAs or *n*-BCMU derivatives (see Figure 1). BCMU solutions are found to exhibit dramatic color changes, from red to yellow or from blue to yellow, when the solvent/nonsolvent ratio or the temperature is increased.^{16,18} In the majority of cases, formation of the blue or red solutions (or suspensions) is followed by precipitation or gel formation.^{18–20} These solvatochromic^{17,19,21–26} and thermochromic^{16,27} transitions have been extensively studied. Additional information on the chromatic properties in conjugated polymers can be found in ref 28.

The origin of the color change of BCMUs has been a point of considerable debate. At the heart of the debate is the fundamental question, is the chromatic transition a purely intramolecular effect or is it an intermolecular effect induced by aggregation of the PDA chains? In the former case, it has been argued that the color change is a result of a backbone conformational change: either a rod-to-coil^{19,21} or planar-to-nonplanar transition.¹⁷ Advocates of the intermolecular process, such as Wegner et al.²² and Hsu et al.,²³ suggested that the solvatochromic

shift was the consequence of aggregation of the wormlike coils present in the yellow solution. Kim et al.²⁹ claimed that the chromatic transitions are primarily a result of changes in the conformational ordering of the polymer backbone and that aggregation only occurs as a secondary consequence of the conformational change. Baughman et al.³⁰ have proposed a different explanation in which the polydiacetylene backbone can adopt an acetylenic or a butatrienic structure, shifting toward the former as the backbone becomes more planar and ordered and the level of electron delocalization increases. However, this model was based on observations of the thermochromic transitions of solid materials, not solutions. It was subsequently applied to solutions but shown to be incorrect by the NMR study of Babbitt and Patel,³¹ who saw no evidence for a cumulenenic structure in yellow solutions. This was confirmed later by others.^{24,32}

The exact nature of the structure and conformation of the backbone and side groups in the yellow, blue, and red solutions and what drives the transition between them still remains unknown. However, evidence exists that the structure and packing of the side groups play an important role in inducing the chromic change. For example, most solutions of *n*-BCMUs having an odd number of methylene groups adjacent to the polymer backbone undergo a change from blue to yellow, while those having an even number of methylenes undergo red to yellow transitions.^{16–18,23,33,34} 1-BCMU is an exception to this odd–even relationship, since it exhibits a red phase at low temperatures.¹⁷ *n*-BCMUs with an odd number of methylene groups can readily adopt a strain-free planar conformation with intramolecular hydrogen bonds between adjacent side groups in the blue phase. In contrast, *n*-BCMUs having an even number of methylene groups can form intramolecular hydrogen bonds only in a slightly twisted, nonplanar conformation.^{34,35} This results in a shorter effective conjugation length than in the planar conformation of

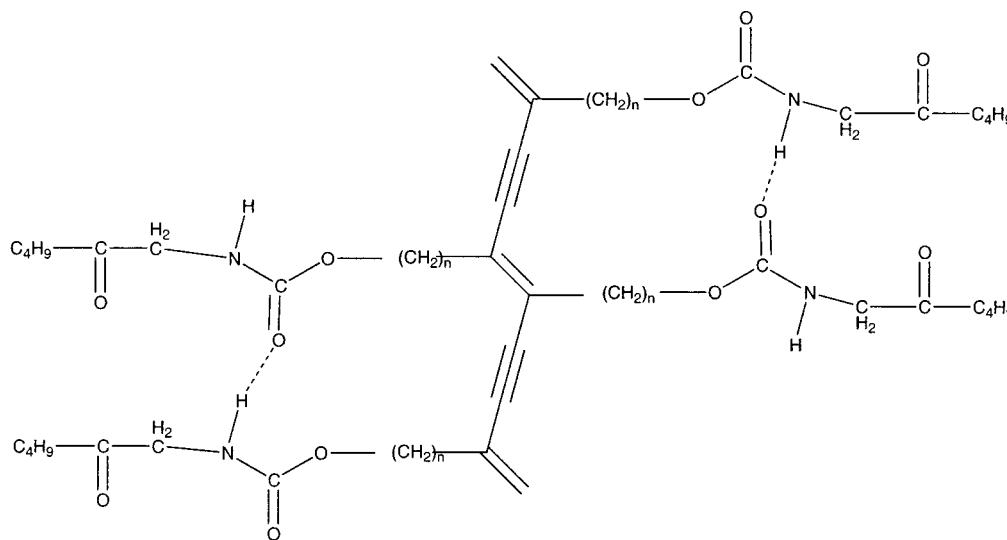


Figure 1. Molecular structure of poly(*n*-butoxycarbonylmethylurethane)-diacetylene. The number of methylenes in the inner alkyl chain of the pendent groups is denoted by *n* (in this work, *n* = 3, 4, 6, or 9). The dashed lines between the carbonyl of one pendent group and the amide group of the other indicate hydrogen bonds.

the blue form. It has been suggested that in the yellow solutions the intramolecular hydrogen bonds are completely broken.^{14,16,18} However, alternative explanations have been presented,^{36,37} and the rupture of hydrogen bonds in the yellow solutions should be considered to be unproven. There is little doubt that the effective conjugation length is substantially smaller in the yellow solutions as a result of static and/or dynamic disorder in the polymer backbone.

The effective average conjugation length of the blue compounds, having the lowest-energy optical transition with a wavelength maximum, λ_{max} , between 600 and 700 nm, has been estimated to be larger than 30 repeat units. The red compounds ($500 \text{ nm} < \lambda_{\text{max}} < 600 \text{ nm}$) have an effective conjugation length between 10 and 20 repeat units, while the yellow structures ($400 \text{ nm} < \lambda_{\text{max}} < 500 \text{ nm}$) have a conjugation length shorter than six repeat units.¹⁷

Recently, Donovan et al.³⁸ have observed ultrafast intramolecular photocurrents on isolated rodlike 4-BCMU chains in toluene at room temperature, while no photocurrent was observed in the coil state at higher temperatures. In the present work, flash-photolysis time-resolved microwave conductivity (FP-TRMC) measurements were performed on *n*-BCMU solutions. The thermotropic behavior of the *n*-BCMU solutions could be followed both optically and by the photoconductivity measurements. The results provide new insights into the optoelectronic properties of these PDAs in the rod and the coil states.

Experimental Section

In Figure 1 the general structure of *n*-butoxycarbonylmethylurethane-PDAs is shown. These polydiacetylene derivatives are commonly called *n*-BCMUs with *n* indicating the number of methylene groups in the intervening alkyl chain. The monomers were synthesized by reacting an isocyanate with a diacetylene diol. The detailed procedure has been described elsewhere.¹⁴ All monomers were recrystallized twice from acetone–hexane mixtures. They were polymerized in the crystalline solid state by ⁶⁰Co γ irradiation at room temperature with dose levels up to 50 Mrad. The molecular weights of the polymers were determined in an earlier study³⁹ and were found to correspond to 1000, 2400, and 4700 monomer units for the 3-BCMU, 4-BCMU, and 9-BCMU, respectively. The molecular weight of the 6BCMU is unknown but is expected

to be between the values for 4-BCMU and 9-BCMU, i.e., approximately 3000 monomer units. Polymer solutions were prepared by adding several milligrams to the UV spectroscopic grade solvents (Fluka) in a 20 mL vessel and placing the vessel in an oven at 70 °C for several hours. The solutions were always stored in the dark to avoid photodegradation.⁴⁰

All *n*-BCMU polydiacetylenes studied were found to be readily soluble in dioxane, resulting in clear, yellow solutions which did not change color on cooling to room temperature. On standing for several days in a refrigerator at ca. 5 °C the 4-BCMU and the 6-BCMU solutions remained clear and yellow. In contrast, the 3-BCMU and 9-BCMU solutions changed to blue and aggregates consisting of small rectangular grains started to form. After several days these aggregates separated from the solution. In the case of 3-BCMU the liquid phase became clear and colorless, while for 9-BCMU it remained blue. After filtering off the aggregates in the latter case, the optical density at 308 nm was less than 0.03, which was too low to carry out quantitative TRMC measurements.

In benzene 4-, 6-, and 9-BCMU could be dissolved at 70 °C to give clear yellow solutions. 3-BCMU could however not be readily dissolved in benzene even at 70 °C. During cooling to room temperature the 4- and 6-BCMU solutions became red. On standing for several days these solutions changed to a red gel phase, which eventually separated from an upper layer of colorless solvent. The 9BCMU solution remained clear and yellow on cooling to room temperature. However, after standing at 5 °C it changed to purple and started to form clearly visible aggregates.

When the solutions, which formed a red gel or blue solid phase on standing at 5 °C for several days, were shaken, they formed suspensions which were optically clear and appeared to be homogeneous to the eye. These red and blue suspensions were relatively stable at room temperature; i.e., they did not revert to yellow solutions, and they showed no signs of phase separation for several hours. These suspensions were the room temperature starting points for the heating and cooling trajectories in the optical absorption and FP-TRMC studies. While their method of preparation clearly indicates that a certain degree of aggregation of the polymer chains almost certainly occurs in the suspensions, they will be loosely referred to as red and blue solutions in the remainder of the text.

Absorption spectra were recorded using a Uvikon 940 UV/vis spectrophotometer. The concentrations were determined, using an extinction coefficient of $17\,500 \text{ L mol}^{-1} \text{ cm}^{-1}$ found for yellow solutions of both 3- and 4-BCMU in chloroform at 468 nm.⁴¹ In the present work concentrations between 1 and 50 μM monomer units were used. Absorption spectra were

subsequently measured on heating and cooling the solutions in a thermostated cuvette.

For flash-photolysis time-resolved microwave conductivity (FP-TRMC) measurements, the solutions were purged with CO₂ to remove air and scavenge any mobile electrons that might be formed in low-yield multiphoton ionization events. The solutions were flash-photolyzed using 7 ns fwhm pulses of 308 nm light from a Lumonics HyperEX 400 excimer laser. A solution of (dimethylamino)nitrostilbene, DMANS, in benzene was used as an internal actinometer.⁴² The maximum power flux per pulse in the cell was approximately 8 mJ cm⁻². This corresponds to approximately 1 absorbed photon per 25 monomer units for the concentrations used.

Any transient change in the photoconductivity of the solution, $\Delta\sigma$, was monitored as a change in the microwave power reflected by a microwave resonant cavity containing the solution. The time response of detection was controlled mainly by the ca. 7 ns time constant of the resonant cavity which had a loaded quality factor, Q_L , of approximately 200. The microwave source was a Gunn diode generating approximately 100 mW at 9 GHz and tunable over the range 8.2–12.4 GHz. The maximum electric field strength within the microwave cavity is related to the loaded quality factor, Q_L , and the incident power level, P_i , by

$$E_0 = \sqrt{\frac{4Q_L P_i \eta}{ab}} \quad [\text{V/m}] \quad (1)$$

In eq 1, a and b are the lengths of the long and short wall sides of the waveguide (2.3 and 1.0 cm, respectively), and η is the impedance of the medium within the cavity, which is given for a TE₁₀ mode by

$$\eta = \frac{377}{\sqrt{\epsilon_r \left[1 - \left(\frac{c}{2af\sqrt{\epsilon_r}} \right)^2 \right]}} \quad [\Omega] \quad (2)$$

with c the velocity of light in vacuo, f the frequency of the microwaves, and ϵ_r the relative dielectric constant of the medium. For a frequency of 9 GHz and $\epsilon_r = 2$, $\eta = 311 \Omega$. Substituting in eq 1 results in

$$E_0 = 2.33 \times 10^3 \sqrt{Q_L P_i} \quad [\text{V/m}] \quad (3)$$

As an example, for typical microwave power levels of 100 mW and a loaded Q of 200, the maximum field strength within the cell is 1.04×10^4 V/m. We have investigated the effect of varying the microwave power from ca. 1 to ca. 40 mW (field strengths from ca. 10 to ca. 70 V cm⁻¹) for solutions of 4-BCMU and 6-BCMU in benzene. No effect was found on the value of the magnitude or the decay kinetics of the conductivity transients.

At the resonance frequency of the cavity the change in the reflected microwave power is related only to changes in the real, or dielectric loss, component of the conductivity of the solution. The transient change in the photoconductivity can be expressed as $\Delta\sigma = eN(t)\Sigma\mu(t)$, with e the elementary charge, $N(t)$ the charge carrier pair concentration at time t , and $\Sigma\mu(t)$ the sum of the hole and electron mobilities. The charge carrier concentration can decrease in time due to recombination, while the mobility can decay in time by relaxation of charge carriers in shallow and/or deep traps. The microwave circuitry, its operation, and the procedure of data analysis have been fully described elsewhere.⁴³

Results

Before discussing the results of the photoconductivity measurements, we present information on the optical properties of the n -BCMU solutions.

Optical Absorption. In dioxane the odd and even BCMUs have very different optical absorption spectra initially; see Figure 2. The spectra of the 4- and 6-BCMU

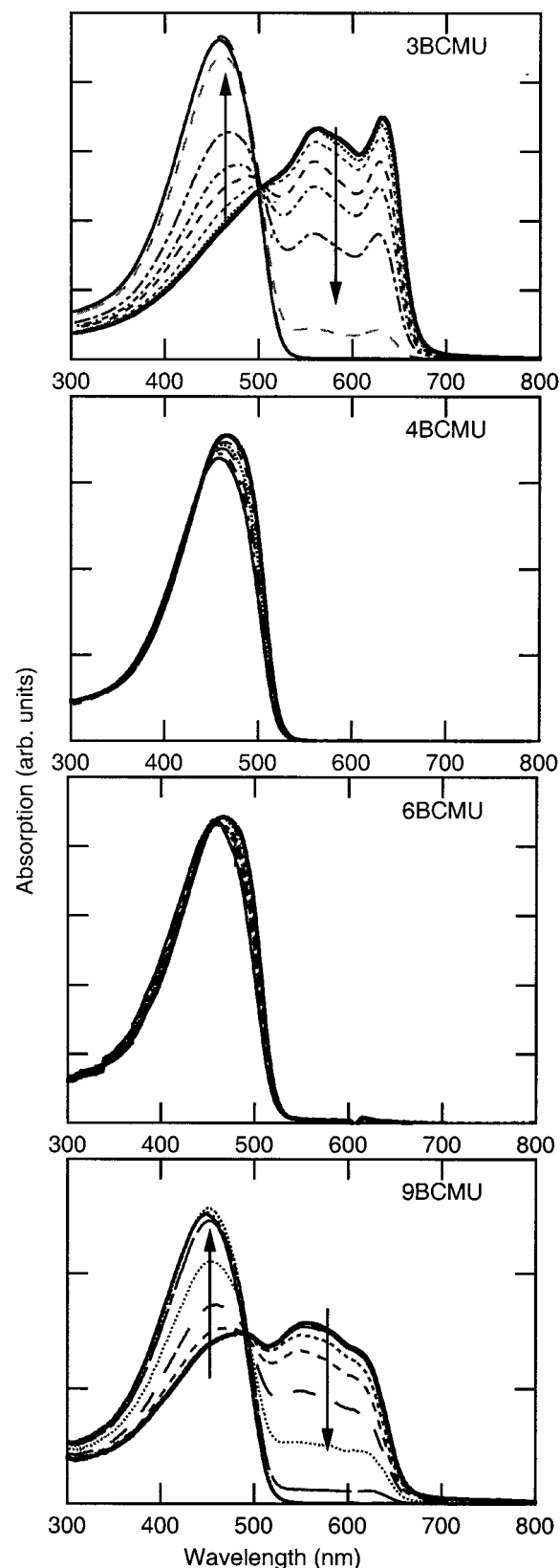


Figure 2. Thermochromic behavior of different n -BCMU PDAs in dioxane. The arrows indicate the direction in which the spectra shift on heating from room temperature (thick solid line). The temperatures used were as follows. 3-BCMU: 20, 26, 33, 39, 45, 50, 57, 63, and 70 °C. 4-BCMU: 20, 30, 41, 47, 55, and 65 °C. 6-BCMU: 20, 26, 33, 39, 45, 54, 60, and 66 °C. 9-BCMU: 20, 25, 29, 34, 39, 42, 47, 54, 64, and 73 °C.

solutions are characterized by a single unstructured absorption band with a maximum at 465 nm (yellow).

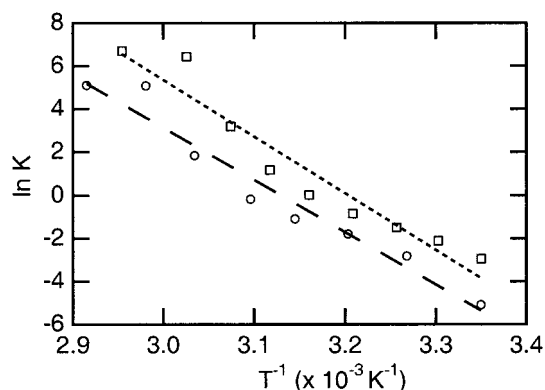


Figure 3. Equilibrium constant, K , plotted logarithmically versus the inverse of the temperature for 3-BCMU (circles) and 9-BCMU (squares) in dioxane. The dashed lines are best linear fits through the data points.

Table 1. Enthalpy and Entropy Differences between the Coil and Rod States

	solvent	$\Delta H_{\text{heating}}$ (eV)	$\Delta S_{\text{heating}}$ (10^{-3} eV K $^{-1}$)
3-BCMU	dioxane (Y/B)	2.1	6.6
9-BCMU	dioxane (Y/B)	2.3	7.4
4-BCMU	benzene (Y/R)	1.8	5.7
6-BCMU	benzene (Y/R)	1.7	5.3

The slight shift to shorter wavelengths with increasing temperature can be attributed to the decrease of the dielectric constant of the solvent. The spectra for the 3- and 9-BCMU solutions are characterized by two absorption bands: one at high temperatures, which is very similar to the 465 nm band found for the even BCMUs, and a broad structured band at low temperatures, which extends to ca. 680 nm. An important observation is the well-defined isosbestic points at ca. 500 nm. This indicates that the two bands correspond to two distinctly separate structures of the polymer chains, which are in thermal equilibrium. These are simply denoted as B (for blue) and Y (for yellow).

From the heights of the long-wavelength spectra, the equilibrium constant, $K = [Y]/[B]$, can be determined. In Figure 3 these values are plotted as $\ln K$ against $1/T$ for 3- and 9-BCMU. From the slopes the values of the enthalpy difference between the two structures, ΔH , can be determined, and these values are listed in Table 1. The values of ca. 2.2 eV are in good agreement with the previous estimate made by Lim et al.¹⁹

For the benzene solutions, the results are somewhat more complicated in that the even BCMUs also display a strong thermochromic effect. The optical absorption spectra of the even BCMUs show two absorption bands: one at high temperatures with a maximum at 465 nm (yellow) very similar to that observed in dioxane solutions and one at 540 nm (red); see Figure 4. Similar to the absorption spectra for 3- and 9-BCMU in dioxane, the shortest wavelength band increases with increasing temperature at the expense of the longer wavelength band. Also, a well-defined isosbestic point is observed, indicating the presence of rodlike and coillike states in thermal equilibrium. The enthalpy differences obtained as for 3- and 9-BCMU in dioxane are listed in Table 1.

The thermochromic behavior of the 9-BCMU solution in benzene is seen to be more complex than that for the even BCMUs presented above. Thus, the initial room temperature spectrum appears to consist of two separate components: one with a sharp maximum at 540

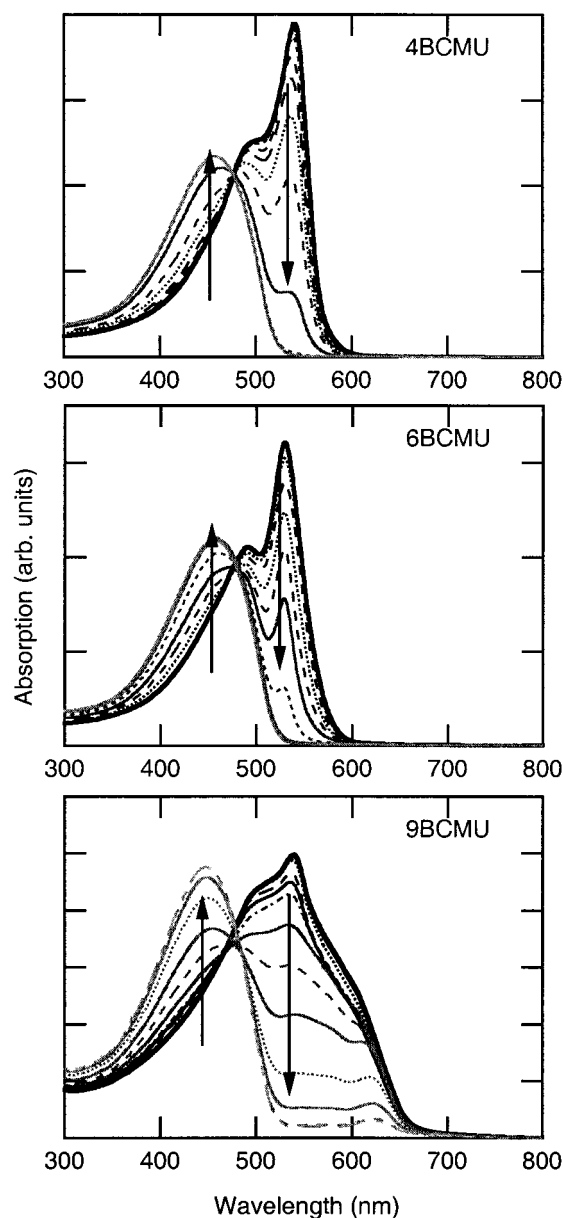


Figure 4. Thermochromic behavior of different n -BCMU PDAs in benzene. The arrows indicate the direction in which the spectra shift on heating from room temperature (thick solid line). The temperatures used were as follows. 4-BCMU: 20, 26, 31, 39, 43, 48, 52, 61, and 66 °C. 6-BCMU: 20, 26, 30, 34, 39, 43, 48, 52, 58, and 66 °C. 9-BCMU: 20, 26, 32, 35, 39, 44, 49, 58, 63, 68, and 72 °C.

nm very similar to that for 4- and 6-BCMU and a much broader band extending to approximately 670 nm, i.e., similar to 9-BCMU at room temperature in dioxane. The former, red band is seen to decrease more rapidly with increasing temperature than the latter. We conclude that two different structures contribute to the initial absorption of the 9-BCMU. Because of this, the transition to the ultimate high-temperature yellow form does not display a well-defined isosbestic point. The initial room-temperature spectrum of 9-BCMU in benzene is identical with that obtained in a 60:40 hexane:chloroform mixture by Bloor et al.⁴⁴

Figure 5 shows the optical density at 550 nm for the different BCMUs in benzene as a function of temperature. As can be seen, a considerable hysteresis is observed.

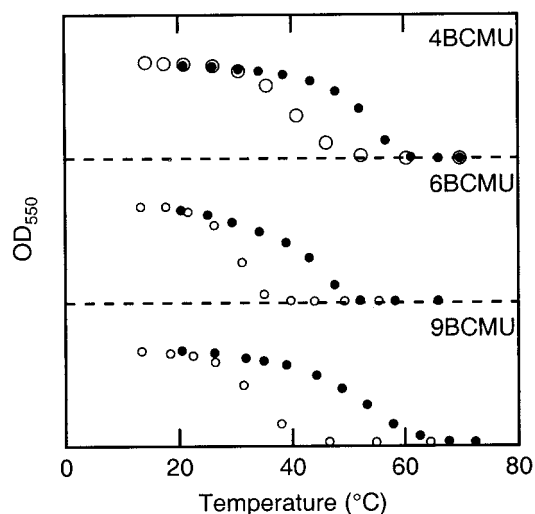


Figure 5. Thermochromic behavior of 4-, 6-, and 9-BCMU in benzene. The filled circles indicate the absorption at 550 nm for a heating cycle and the open circles for a cooling cycle.

Photoconductivity. In Figure 6 photoconductivity transients are shown for the *n*-BCMU solutions in dioxane at room temperature. A marked difference can be seen between the odd and even BCMU solutions. Photoexcitation of the blue solutions of 3- and 9-BCMU yields readily measurable, long-lived conductivity transients, while flash photolysis of the yellow solutions of 4- and 6-BCMU results in a very small short-lived change in the photoconductivity. Yellow solutions of 3- and 9-BCMU could be prepared at room temperature by cooling an initially hot solution. These solutions also displayed no significant photoinduced conductivity transients as was also found for the yellow 4- and 6-BCMU solutions. The results obtained for the 4-, 6-, and 9-BCMU solutions at room temperature in benzene are presented in Figure 7. All three solutions are seen to yield readily measurable long-lived photoconductivity transients.

In Figure 8 the temperature dependence of the photoconductivity is presented for a solution of 4-BCMU in benzene. The measured conductivity decreases upon heating, and at approximately 60 °C it has practically vanished. In Figure 9 the maxima of the conductivity transients from Figure 8 are shown at different temperatures together with the optical absorption of the same solution at 545 nm. The decrease in photoconductivity on heating and increase on cooling are seen to closely follow the changes in the 545 nm absorption corresponding to the red form of the polymer. Similar results were found for the 6- and 9-BCMU in benzene and the 3- and 9-BCMU in dioxane.

As mentioned in the Experimental Section, the transient change in the conductivity is given by $\Delta\sigma = eN(t)\Sigma\mu(t)$. The charge carrier concentration is equal to $N(t) = N_{\text{abs}}\phi_p S(t)$, with N_{abs} the number of absorbed photons per unit volume, ϕ_p the quantum efficiency for charge carrier generation, and $S(t)$ the fraction of charge carriers that has survived recombination at time t . Since $S(t) \leq 1$ and $\Sigma\mu(t) \leq \Sigma\mu(t=0)$, the value of $\Delta\sigma/eN_{\text{abs}}$ at the end of the laser pulse provides a lower limit of $\phi_p\Sigma\mu$ at zero time. In Table 2 the values of $\phi_p\Sigma\mu$ obtained from the conductivity in Figures 6 and 7 at the end of the laser pulse are given for the different BCMUs in dioxane and benzene at room temperature.

To obtain detailed insight into the decay kinetics of the photoconductivity, the measurements on 4-BCMU

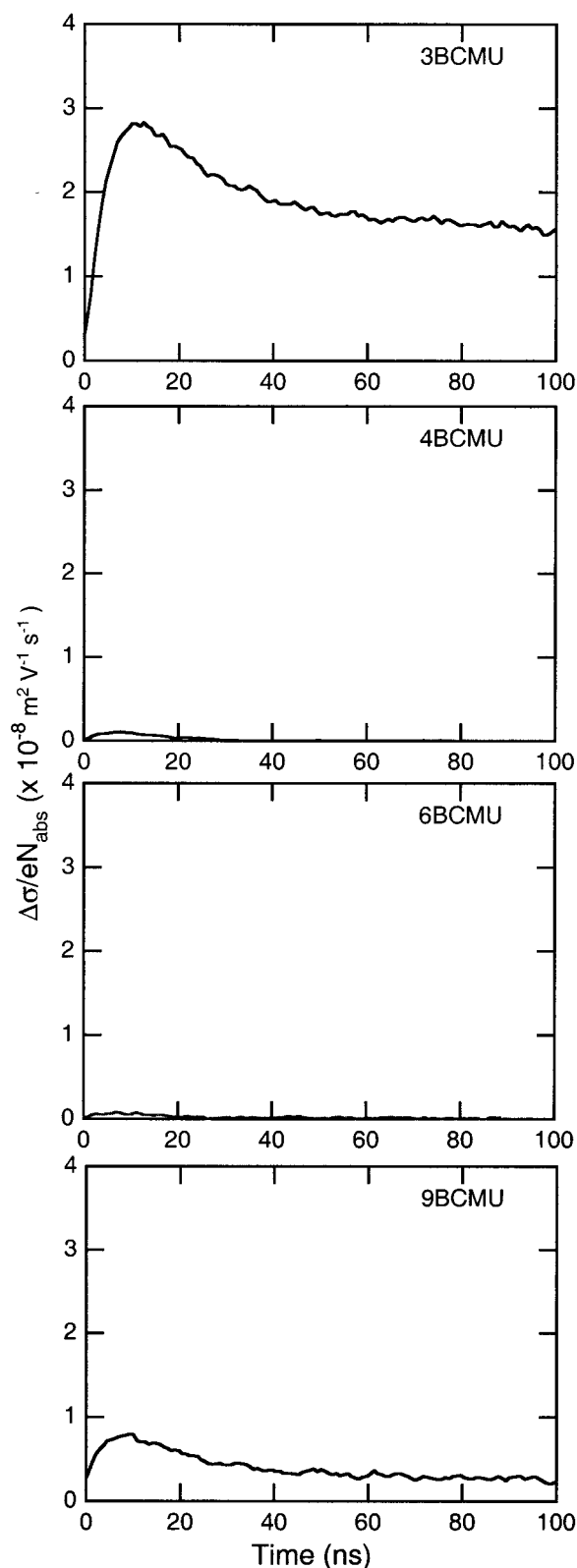


Figure 6. Transient changes in the photoconductivity on flash photolysis of *n*-BCMU solutions in dioxane at room temperature.

solutions in benzene were extended to longer time scales and lower light intensities. The light intensity normalized photoconductivity transients are plotted double logarithmically in Figure 10. The decay of the conductivity transients after the initial growth during the pulse is seen to be approximately linear on this double-logarithmic representation, indicating an inverse power-

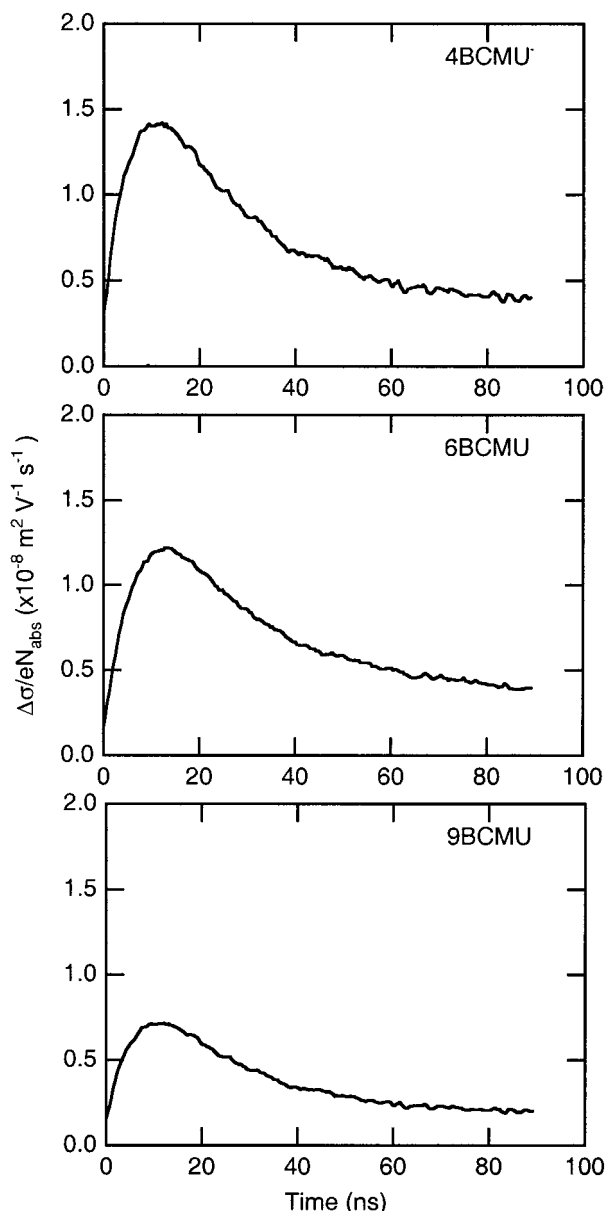


Figure 7. Transient changes in the photoconductivity on flash photolysis of *n*-BCMU solutions in benzene.

law time dependence, i.e., $\Delta\sigma \propto 1/t^\alpha$. The dashed straight line in Figure 10 corresponds to $\alpha = 0.34$.

Discussion

Optical Absorption. The thermochromic behavior of *n*-BCMUs in dioxane and benzene shown in Figures 2 and 3 is similar to results obtained in other solvents^{16,19,22} and solvent mixtures.²³ Three states can be distinguished, characterized by yellow, red, and blue colors. The enthalpies of formation of the blue and red forms from the yellow form of -2.2 and -1.8 eV, respectively, indicate that the blue form is energetically the most stable of the three. The broad structureless spectrum of the yellow form is attributed to a coil-like configuration of the polymer backbones with relatively short conjugation lengths. The red and blue forms are considered to result from the adoption of a more planar backbone structure with a higher degree of conjugation. Both long-wavelength forms display well-defined structure in their absorption bands indicative of coupling between the electrons and the vibrational modes of the

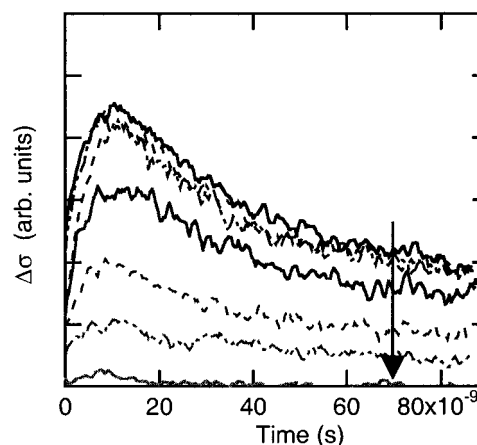


Figure 8. Photoconductivity transients for 4-BCMU in benzene upon heating. The arrow indicates the heating cycle going from room temperature to higher temperatures. The upper solid line was recorded at room temperature (24°C); the other transients were measured at 33 , 41 , 46 , 52 , 56 , and 60°C .

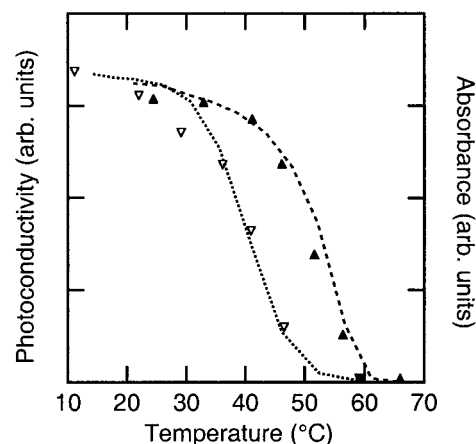


Figure 9. Temperature dependence of the photoconductivity on heating (\blacktriangle) and cooling (∇) starting with 4-BCMU in benzene. The dashed and dotted curves represent the optical absorption at 545 nm on heating and cooling, respectively (analogous to data in Figure 4).

Table 2. $\phi_p \Sigma \mu$ (Product of the Quantum Yield for Charge Carrier Generation and the Sum of the Charge Carrier Mobilities) Determined at the End of the Laser Pulse for Different BCMU Dioxane or Benzene Solutions at Room Temperature

PDA derivatives	dioxane		benzene	
	color	$\phi_p \Sigma \mu (\times 10^{-4} \text{ cm}^2 \text{ V}^{-1} \text{ s}^{-1})$	color	$\phi_p \Sigma \mu (\times 10^{-4} \text{ cm}^2 \text{ V}^{-1} \text{ s}^{-1})$
3-BCMU	B	3.0 ± 0.5		
	Y	0.05 ± 0.02		
4-BCMU	Y	0.07 ± 0.03	R	1.4 ± 0.2
6-BCMU	Y	0.07 ± 0.03	R	1.1 ± 0.2
9-BCMU	B	0.8 ± 0.2	B/R	0.8 ± 0.2
	Y	0.05 ± 0.02		

polymer backbone and only a narrow distribution of conjugation lengths.

In the case of the yellow forms there is little doubt that true solutions are formed with the polymer chains isolated from each other. The blue and red forms however form solid precipitates and gels, respectively, on standing, and their method of preparation in the present work makes it almost certain that these are suspensions of at least partially aggregated polymer chains rather than solutions of isolated polymer chains. The overall spectral characteristics, thermodynamics,

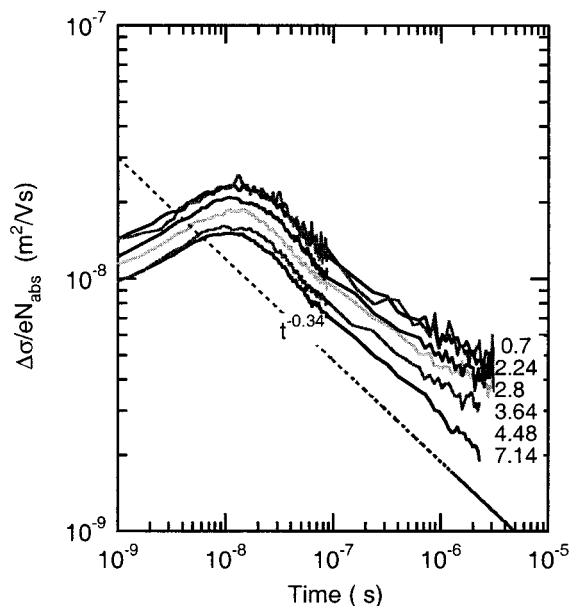


Figure 10. Light intensity normalized photoconductivity transients for a 4-BCMU solution in benzene plotted double logarithmically for five different excitation energy fluxes (given in mJ cm^{-2}). The initial rise below 10 ns is due simply to the increase in conductivity occurring during the laser pulse. The dashed line corresponds to an inverse power law dependence.

and type of aggregation (i.e., solid versus gel) indicate that the planarity of the backbone and the conjugation length are greater in the blue form. Both red and blue forms do however appear to have a very regular, rodlike backbone structure as evidenced by the sharpness of the vibrational bands in both cases. The appearance of both blue and red states together in 9-BCMU¹⁷ has been found previously in a 60:40 hexane:chloroform mixture by Bloor et al.⁴⁴ The latter work also shows solutions with the “pure” blue and red forms and discussed the dependence of the polymer structure on solvent. The blue form shows distinct Raman spectra close to those of the initial crystalline materials,^{45,46} which agrees with the observation of crystallites in the blue BCMU solutions. The red form has been found to have Raman spectra with very similar frequencies for the double and triple stretching modes for a variety of polydiacetylenes.^{45,46} Thus, the backbone structures would appear to be very similar despite differences in side group structure.

Photoconductivity. The most prominent characteristic of the photoconductivity of the BCMU solutions studied is the complete contrast between the yellow solutions, which display an extremely small, short-lived conductivity, and the red and blue solutions for which large, long-lived conductivity transients are observed. The differences observed could be ascribed to the influence of the backbone conformation on the mobility of the charge carriers formed. Thus, the static and dynamic backbone disorder of the yellow form, as evidenced by its broad structureless absorption spectrum, would be expected to result in a considerably lower mobility than the more extended backbone conjugation and rigidity associated with the red and blue forms.

However, the possibility cannot be completely dismissed that the difference is a result of aggregation which undoubtedly (eventually) occurs in the case of the longer wavelength forms but is definitely absent in the

case of the yellow solutions. The readily observable transients observed in the former “solutions” could then be ascribed to the occurrence of interchain exciton dissociation within aggregated chain segments, resulting in an electron and hole on separate polymer chains. This could retard the rapid geminate recombination of charges that would take place on isolated chains.

Donovan et al. purported that in their experiments the chains were isolated even for the red solutions of 4-BCMU. In our case it is quite certain that aggregation must be present in the initial red and blue solutions investigated because of the method of preparation. However, in the temperature study of 4-BCMU shown in Figure 9, the conductivity signal was found to return precisely to the level found for the initial solution when it was cooled. Since the cooling took place over a period of minutes while visual evidence of gel formation, even on standing at 5 °C, takes several hours, it is presumed that much less chain aggregation was present in the freshly cooled solution while the photoconductivity was unchanged. This would therefore suggest that the large conductivity transients observed for the red form are in fact mainly due to the higher mobility of the charge carriers rather than to an interchain mechanism of formation. It has however been clearly demonstrated, in identical TRMC experiments on a benzene solution of a phenylene–vinylene polymer, that chain aggregation can result in an order of magnitude larger photoconductivity transients as a result of interchain exciton dissociation.^{47,48}

Differentiation between the red and the blue forms of the present BCMUs is more difficult since the values of $\phi_p \Sigma \mu$ all lie within the range 0.8×10^{-4} – $3 \times 10^{-4} \text{ cm}^2/(\text{V s})$ for $\phi_p \Sigma \mu$ with the two blue solutions of 9-BCMU lying at the bottom of the range and the blue solution of 3-BCMU in dioxane at the top. On comparing the optical spectra, it is apparent that the vibrational fine structure for 9-BCMU is substantially broader than for 3-BCMU. This is taken to indicate that the polymer backbone in the latter case has a more uniform structure. Therefore, the higher value of $3 \times 10^{-4} \text{ cm}^2/(\text{V s})$ for $\phi_p \Sigma \mu$ is associated with a well-defined planar, all-trans configuration. The vibrational bands in the red solution spectra of 4-BCMU and 6-BCMU in benzene are very similar to each other and also similar in width to that for the blue 3-BCMU solution in dioxane. The somewhat lower values of $\phi_p \Sigma \mu$ for the “red” compounds, i.e., 1.4×10^{-4} and $1.1 \times 10^{-4} \text{ cm}^2/(\text{V s})$, are therefore considered to be a result of the shorter conjugation length resulting from a lack of perfect coplanarity in what is otherwise a well-defined, all-trans backbone structure. In agreement with this, the photoconductivity is found to be lower in red as opposed to blue forms of diacetylenes also in thin films which can be converted from blue to red in the solid state by high-temperature annealing. Similar results on a film of another polydiacetylene derivative were reported recently by Savenije et al.⁴⁹

Decay Kinetics. As can be seen from Figure 7, a substantial decay of the photoconductivity transients occurs over a time scale of tens of nanoseconds following the laser pulse. This is still much longer however than the very rapid, nanosecond decay time found in the recent DC flash photoconductivity study of 4-BCMU in toluene by Donovan et al.³⁸ However, the laser pulse width in our measurements was 7 ns, i.e., much longer than the 25 ps used in ref 38. In addition, the rise time

of detection was an order of magnitude longer than the 700 ps of the previous work. These two facts combined help to explain, at least in part, why we were unable to observe the very rapid decay process observed in that work. Another factor that might contribute to a difference between the decay kinetics is the much higher intensity (in photons/cm²/s) used in the work of Donovan et al.³⁸ In Figure 10 the gradual decrease in the magnitude of the transients and increase in the decay rate with increasing laser pulse intensity indicates that charge recombination becomes more important as the initial charge carrier concentration increases. However, for the two lowest intensities used, the difference in the decay is not very large, and therefore at these intensities it can be assumed that charge recombination does not play a dominant role.

The decay kinetics at long times can be well described by a $t^{-\alpha}$ law (with $\alpha = 0.34 \pm 0.04$). Note that this value of α is much lower than the value close to unity found by Movaghar et al.⁵⁰ in PTS crystals. Alternatively, Hunt et al.⁵¹ and Rughooputh et al.⁵² found that the charge carrier decay in PDA-10H crystals could well be described by an $\exp(-bt^{1/3})$ law, which is characteristic of deep trapping in a one-dimensional system.

A power-law dependence of the decay of the mobility is characteristic for a thermally activated hopping motion in a disordered energy landscape with shallow traps with an exponential distribution of their depths.^{53–56} In such an energy landscape each localization site of the charge carrier can act as a temporary trap. The dwell time in a trap increases with the depth. As time proceeds, it becomes more likely that a charge carrier has encountered a deeper trap, and consequently the mobility of the charge carrier decreases with time.

For times exceeding the inverse of the average frequency for hopping between adjacent traps and for a sufficiently small external electric field, the relaxation of the charge carrier mobility in an energy landscape with an exponential trap distribution can be described by the inverse power law (see eq 22 in ref 56)

$$\mu(t) = \frac{ew_0a^2A}{(w_0t)^\alpha} \quad (4a)$$

with

$$\alpha = \frac{T_0 - T}{T_0 + T} \quad (4b)$$

In eq 4 e is the electronic charge, w_0 is the attempt frequency for hopping, a is the jump distance between adjacent traps, T is the temperature, and $k_B T_0$ is the average trap depth with k_B the Boltzmann constant. The factor A in eq 4a depends on the average trap depth and the temperature; see ref 56. Note that eq 4 is only valid for an electric field strength $E \leq k_B T/(ea)$. As discussed in the Experimental Section, the maximum electric field strength in the experiments is $E = 10^4$ V/m. This field strength is sufficiently low for eq 4 to be applicable for jump distances less than 2.5 μ m, which corresponds to 5000 monomer units. According to eq 4, the slope of the decay of the conductivity in Figure 10 (i.e., the value of α) is entirely determined by the average trap depth $k_B T_0$. As discussed above, the experimental results yield $\alpha = 0.34 \pm 0.04$, which corresponds to an average trap depth of 0.05 \pm 0.005 eV.

Conclusions

n-Butoxycarbonylmethylurethane-polydiacetylenes, *n*-BCMU-PDAs, undergo thermochromic and solvatochromic transitions in solution. Odd BCMUs exhibit a rod-to-coil transition visualized by blue to yellow color changes, while the even BCMUs change from red to yellow. The rod state (blue and red) is metastable and reverts to a gellike form in the case of the red state, while the blue state forms crystallites, which eventually precipitate. These rod-to-coil transitions can be followed by optical absorption of the solutions. The observation of the coexistence of both a blue and a red form for 9-BCMU in benzene is exceptional.

Photoexcitation of BCMU solutions in the rod state results in a large transient change in the photoconductivity as monitored using the time-resolved microwave conductivity (TRMC) technique, while hardly any signal can be observed in the coil state (in dioxane). The thermochromic shift going from the rod state at room temperature to the coil state at 65 °C could be followed by measuring the conductivity, which showed a gradual decrease with temperature close to that found for the long-wavelength optical absorption. The large conductivity signal in the rod state is attributed to the formation of mobile charge carriers via interchain charge transfer in the aggregate, resulting in the predominant formation of charge carriers located on different chains. The lower limit of the product of the quantum efficiency for charge carrier formation, ϕ_p , and the sum of the charge carrier mobilities, $\Sigma\mu$, is found to be $\phi_p \Sigma\mu = (1.2 \pm 0.2) \times 10^{-4}$ cm² V⁻¹ s⁻¹ for the red state, while a slightly larger value of $(3.0 \pm 0.5) \times 10^{-4}$ cm² V⁻¹ s⁻¹ was found for the blue state.

The conductivity signal eventually decays during time according to a power law with a power $\alpha = 0.34 \pm 0.04$. This observation suggests a decay of the charge carrier mobility as a consequence of their motion in a disordered energy landscape with shallow traps. The experimental decay could be described assuming an exponential distribution of trap depths with an average depth of 0.05 \pm 0.005 eV.

References and Notes

- (1) Wegner, G. Z. *Naturforsch.* **1969**, *24B*, 824.
- (2) Chance, R. R.; Baughman, R. H.; Müller, H.; Eckhardt, C. J. *J. Chem. Phys.* **1977**, *67*, 3616.
- (3) Tieke, B.; Lieser, G.; Wegner, G. *J. Polym. Sci., Polym. Chem.* **1979**, *17*, 1631.
- (4) Kanetake, T.; Tokura, Y.; Koda, T. *Solid State Commun.* **1985**, *56*, 803.
- (5) Tokura, Y.; Kanetake, T.; Ishikawa, K.; Koda, T. *Synth. Met.* **1987**, *18*, 407.
- (6) Ishikawa, K.; Fukagai, K.; Kanetake, T.; Koda, T.; Tokura, Y.; Koshihara, S. *Synth. Met.* **1989**, *28*, D605.
- (7) Sauteret, C.; Hermann, J. P.; Frey, R.; Pradère, F.; Ducuing, J.; Baughman, R. H.; Chance, R. R. *Phys. Rev. Lett.* **1976**, *36*, 956.
- (8) Carter, G. M. *J. Opt. Soc. Am. B* **1987**, *4*, 1018.
- (9) Kanetake, T.; Ishikawa, K.; Hasegawa, T.; Koda, T.; Takeda, K.; Hasegawa, M.; Kubodera, K.; Kobayashi, H. *Appl. Phys. Lett.* **1989**, *54*, 2287.
- (10) Nakanishi, H.; Matsuda, H.; Kato, M. *Mol. Cryst. Liq. Cryst.* **1984**, *105*, 77.
- (11) Se, K.; Ohnuma, H.; Kotaka, T. *Macromolecules* **1984**, *17*, 2126.
- (12) Bhattacharjee, H. R.; Preziosi, A. F.; Patel, G. N. *J. Chem. Phys.* **1980**, *73*, 1478.
- (13) Bhattacharjee, H. R.; Preziosi, A. F.; Patel, G. N. *J. Polym. Sci., Polym. Symp.* **1984**, *71*, 259.
- (14) Patel, G. N. *Polym. Prepr. (Am. Chem. Soc., Div. Polym. Chem.)* **1978**, *19*, 154.

- (15) Patel, G. N.; Walsh, E. K. *J. Polym. Sci., Polym. Lett. Ed.* **1979**, *17*, 203.
- (16) Patel, G. N.; Witt, J. D.; Khanna, Y. P. *J. Polym. Sci., Polym. Phys.* **1980**, *18*, 1383.
- (17) Patel, G. N.; Miller, G. G. *J. Macromol. Sci., Phys. B* **1981**, *20*, 111.
- (18) Patel, G. N.; Chance, R. R.; Witt, J. D. *J. Chem. Phys.* **1979**, *70*, 4387.
- (19) Lim, K. C.; Heeger, A. J. *J. Chem. Phys.* **1985**, *82*, 522.
- (20) Lim, K. C.; Kapitulnik, A.; Zacher, R.; Heeger, A. J. *J. Chem. Phys.* **1985**, *82*, 516.
- (21) Lim, K. C.; Fincher, C. R. J.; Heeger, A. J. *Phys. Rev. Lett.* **1983**, *50*, 1934.
- (22) Rawiso, M.; Aime, J. P.; Fave, J. L.; Schott, M.; Müller, M. A.; Schmidt, M.; Baumgarten, H.; Wegner, G. *J. Phys. (Paris)* **1988**, *49*, 861.
- (23) Coyne, L. D. D.; Chang, C.; Hsu, S. L. *Macromol. Chem.* **1987**, *188*, 2311.
- (24) Nava, A. D.; Thakur, M.; Tonelli, A. E. *Macromolecules* **1990**, *23*, 3055.
- (25) Rosenblatt, C.; Rubner, M. F. *J. Chem. Phys.* **1989**, *91*, 7896.
- (26) Chu, B. Xu, R. *Acc. Chem. Res.* **1991**, *24*, 384.
- (27) Takeda, K.; Hasegawa, M.; Koshihara, S.; Tokura, Y.; Koda, T. *Mol. Cryst. Liq. Cryst.* **1990**, *183*, 371.
- (28) Batchelder, D. N. *Contemp. Phys.* **1988**, *29*, 3.
- (29) Kim, W. H.; Kodali, N. B.; Kumar, J.; Tripathy, S. K. *Macromolecules* **1994**, *27*, 1819.
- (30) Baughman, R. H.; Chance, R. R. *Ann. N. Y. Acad. Sci.* **1978**, *313*, 705.
- (31) Babbitt, G. E.; Patel, G. N. *Macromolecules* **1981**, *14*, 554.
- (32) Campbell, A. J.; Davies, C. K. L. *Polymer* **1995**, *36*, 675.
- (33) Peiffer, D. G.; Chung, T. C.; Schulz, D. N.; Agarwal, P. K.; Garner, R. T.; Kim, M. W. *J. Chem. Phys.* **1986**, *85*, 4712.
- (34) Brown, A. J.; Rumbles, G.; Phillips, D.; Bloor, D. *Chem. Phys. Lett.* **1988**, *151*, 247.
- (35) Chance, R. R.; Patel, G. N.; Witt, J. D. *J. Chem. Phys.* **1979**, *71*, 206.
- (36) Chang, C.; Hsu, S. L. *Makromol. Chem.* **1985**, *186*, 2557.
- (37) Walters, G.; Painter, P.; Ika, P.; Frisch, H. *Macromolecules* **1986**, *19*, 888.
- (38) Donovan, K. J.; Hargrave, P.; Scott, K.; Somerton, M.; Spagnoli, S. *Phys. Rev. Lett.* **1998**, *81*, 3731.
- (39) Van der Laan, G. P.; De Haas, M. P.; Warman, J. M.; De Leeuw, D. M.; Tsibouklis, J. *ACS Symp. Ser.* **1994**, *549*, 316.
- (40) Bloor, D.; Worboys, M. R. *J. Mater. Chem.* **1998**, *8*, 903.
- (41) Patel, G. N.; Khanna, Y. P.; Ivory, D. M.; Sowa, J. M.; Chance, R. R. *J. Polym. Sci., Polym. Phys. Ed.* **1979**, *17*, 899.
- (42) Schuddeboom, W. Ph.D. Thesis ISBN 90-73861-21-7, Delft University of Technology 1994.
- (43) De Haas, M. P.; Warman, J. M. *Chem. Phys.* **1982**, *73*, 35.
- (44) Bloor, D.; Ando, D. J.; Obhi, J. S.; Mann, S.; Worboys, J. R. *Makromol. Chem. Rapid Commun.* **1986**, *7*, 665.
- (45) Campbell, A. J.; Davies, C. K. L.; Batchelder, D. N. *Macromol. Chem. Phys.* **1998**, *199*, 109.
- (46) Bloor, D. *Polymer* **1999**, *40*, 3901.
- (47) Gelinck, G. H.; Warman, J. M.; Staring, E. G. J. *J. Phys. Chem.* **1996**, *100*, 5485.
- (48) Gelinck, G. H.; Staring, E. G. J.; Hwang, D.-H.; Spencer, G. C. W.; Holmes, A. B.; Warman, J. M. *Synth. Met.* **1997**, *84*, 595.
- (49) Savenije, T. J.; Warman, J. M.; Barentsen, H. M.; van Dijk, M.; Zuilhof, H.; Sudhölter, E. J. R. *Macromolecules* **2000**, *33*, 60.
- (50) Movaghar, B.; Murray, D. W.; Donovan, K. J.; Wilson, E. G. *J. Phys. C: Solid State Phys.* **1984**, *17*, 1247.
- (51) Hunt, G.; Bloor, D.; Movaghar, B. *J. Phys. C: Solid State Phys.* **1985**, *18*, 3497.
- (52) Rughooputh, S. D. D. V.; Bloor, D.; Phillips, D.; Movaghar, B. *Phys. Rev. B* **1987**, *35*, 8103.
- (53) Monroe, D.; Orenstein, J.; Kastner, M. *J. Phys. (Paris)* **1981**, *42*, 553.
- (54) Schönherr, G.; Bäessler, H.; Silver, M. *Philos. Mag. B.* **1981**, *44*, 47.
- (55) Siebbeles, L. D. A.; Berlin, Y. A. *Chem. Phys. Lett.* **1997**, *265*, 460.
- (56) Berlin, Y. A.; Siebbeles, L. D. A.; Zharikov, A. A. *Chem. Phys. Lett.* **1999**, *305*, 123.

MA000485B